6.1 CAN URBAN OZONE GENERATION BE MODELED CORRECTLY BASED ON MAJOR GASEOUS ATMOSPHERIC REACTIONS?

A. Gholizadeh, Damon Matthews, Mitra Bahri, and Mahsa Madani Hosseini
Concordia University, Montreal, Quebec

1. Introduction

Urban areas have been developing rapidly in recent years (United Nation Information Service, 2004). Predictions show a much faster urbanization trend for the near future that will result in the settlement of more than 5 billion residents in metropolitan areas by 2030. This growth in population and number of cities is causing many problems on the air quality of those areas (Alba Webb, Parmenter, Allen, & Mc Donald-buller, 2008,; Song, Parmenter, McDonald-Buller, Allen, & T.; Duh, Shandas, Chang, & George, 2008; Moore, Gould, & Keary, 2003; Li, Li, Zhou, Shi, & Zhu, 2012). Air pollution is defined as an undesirable quantity of atmospheric constituents that causes harm to humans or our surroundings (EPA, Community Air Screening How to- Manual, 2004). Increase in ground-level ozone concentration is reported to be very harmful to human respiratory organs (Canadian Centre for Occupational Health and Safety, 1998). This problem can be resolved by acquiring proper environmental and technical solutions. However, solutions need legislation and effective policies to achieve acceptable results (Soubbotina & Sheram, 2000). In order to propose a proper air quality model, pollutants with major concern should be verified. There are six different air pollutants that have main concerns for United States Environmental Protection Agency (EPA); including carbon monoxide (CO), lead (Pb), nitrogen dioxide(NO_2), ozone (O_3), particulate matter (PM) and sulfur dioxide (SO_2) (EPA, Air Pollution Emissions Overview, 2011). Among these pollutants, ozone is of more interest due to its generation dependence on temperature. Unlike the other pollutants, temperature has a direct and substantial effect on the ozone generation by chemical reactions.

While most pollutants are emitted directly, some are secondary product of reactions between primary pollutants, such as NO_X and hydroperoxyl. Furthermore, those reactions that produce the secondary pollutants strongly depend on the ambient condition. Hence, different pollutants may be observed in different times of a year or during a day. Unlike other gaseous pollutants, ozone, as a secondary product pollutant, has higher concentration in summertime (Table 1). It is also expected to have a high concentration of ozone in the afternoon (Zeldin & Meisel, 1978) by the secondary reactions. In order to be able to track different reactions in the model, major groups of atmospheric constituents are introduced. Based on Seinfeld et al. (Seinfeld & Pandis, 2006), there are four major groups of atmospheric constituents in urban areas; including sulfur-containing compounds, nitrogen-containing compounds, carbon-containing compounds, and halogen-containing compounds.

Pollutant	Spring	Summer	Fall	Winter
SO_x	Medium	Low	Medium	High
NO_x	Medium	Low	Medium	High
CO	Medium	Low	Medium	High
O_3	Medium	High	Medium	Low

Table 1: Qualitative comparison of concentration of gaseous pollutants (Zeldin & Meisel, 1978) **in different seasons**

Ozone concentration quantity, in different regions around the world, is reported in the literature based on simulations and experimental data (see (Baldwin, Barker, Golden, & Hendry, 1977; Dickerson, et al., 1997 ; Carter, Wine, Darnall, & N. Pitts, 1979) and the references therein). Baldwin et al. (Baldwin, Barker, Golden, & Hendry, 1977), Dickerson et al. (Dickerson, et al., 1997), and Carter et al. (Carter, Wine, Darnall, & N. Pitts, 1979) investigated the relationship of the temperature increase in summertime to ozone generation. Walcek et al. (Walcek & Yuan, 1994) improved the simulation methodology to study effects of the temperature increase on the ozone concentration. They considered reactions of both organic and inorganic compounds to explore the sensitivity of them to different meteorological parameters. Finally, they concluded that the increase in the temperature results in more ozone pollution (Walcek & Yuan, 1994). Other researches performed simulations to identify the consecutive effect of albedo increase, in urban areas, on ozone generation (Taha, 1997). They also reported ozone decrease by reduction of sunlight energy absorption in the urban areas of the US south coast air basin. In a project in Greece, researchers evaluated the ozone concentration and the temperature quantity using experimental data recorded in different locations of Athens

*Corresponding author: 1455 de Maisonneuve Blvd. West EV014.169, Montreal, Quebec, Canada H3G 1M8, Tel: 514-848-2424 X7039 Email: Ali.gholizade@gmail.com

(Stathopoulou, Mihalakakou, Santamouris, & Bagiorgas, 2008). They concluded that there was a linear correlation between the ozone concentration and the temperature. Moreover, a smooth change in the ozone concentration compared to the temperature variation was observed. Other researchers studied the relationship experimentally, based on ozone reactions in bench scale reactor with different gaseous baths (see (Hippler, Rahn, & Troe, 1990; Atkinson, et al., 2004), and the references therein). Accordingly, different advanced models have been developed to simulate chemical reactions in the atmosphere. Some coupled chemistry-meteorological models are able to consider meteorological variables as the inputs to determine feedbacks of the system (Jacobson M. Z., 2001; Jacobson M. Z., 2001; Wu, et al., 2007; Eyring & et al., 2006). Many of these models are used to find the ozone concentration, considering all effective variables. However, these models are too complex to provide sensitivity analysis of the response of the ozone generation to temperature, anthropogenic emission, and trace gases. Hess et al. (Hess, Carnovale, Cope, & Johnson, 1992) reported the effect of the temperature and initial compositions on four reaction mechanisms. It is still demanding to find a simple model to track ozone response to variations of its inputs. For the sake of simplicity, one can consider more effective parameters and neglect inorganic reactions. The main objective of this paper is to use STELLA software to propose a simple model for simulating the ozone concentration variation. Investigating the sensitivity of ozone concentration to temperature is another aspect of this study.

2. Theory

In this section, first, we introduced governing equations that affect meteorological parameters. Then, reaction rates and parameterization methods of different types of atmospheric reactions of the model discussed. Thereafter, important reactions that were used in the model presented.

2.1. Governing equations

Governing equations of the model are mainly based on the conservation laws of mass, momentum, and energy. Physical interpretation of the conservation laws for our model can be written as:

$$\binom{generation\ of}{pollutants} - \binom{Dissipation\ of}{pollutants} + \binom{Inflow\ of}{pollutants} - \binom{Outflow\ of}{pollutants} = \binom{Accumulation\ of}{pollutants}$$

Generation of pollutants consists of anthropogenic emission and chemical reactions, whereas, dissipation mechanisms comprise deposition mechanism (dry and wet) and chemical reactions.

2.2. Atmospheric reactions and reaction rates

There are hundreds of gaseous constituents in the troposphere, where different types of reactions take place. Reactions of the model were categorized in four major groups of photochemical, oxygen, nitrogen, and carbon reactions. In this paper, main focus was in the rate of the reactions, for photochemical reactions that require solar energy and other three groups of the chemical reactions. Hence, methods of parameterization of the reactions were discussed first and then reactions were introduced.

2.2.1. Parameterization of reaction rates

For a simple reaction

$$\tilde{A} + \tilde{B} \xrightarrow{k} \tilde{C}$$

the rate of generation and dissipation of each component can be calculated from:

$$\frac{d\tilde{A}}{dt} = \frac{d\tilde{B}}{dt} = \frac{d\tilde{C}}{dt} = k[\tilde{A}][\tilde{B}]$$

The reaction rate, *k*, can be determined by the collision theory as shown in Eq (6) (Seinfeld & Pandis, 2006).

$$k = Ae^{-\frac{E}{RT}} \quad (6)$$

For photolysis reaction like

$$\tilde{A} + h\nu \xrightarrow{j} \tilde{B}$$

The rate of dissipation of $\tilde{A}$ (or rate of generation of $\tilde{B}$) is

$$\frac{d\tilde{A}}{dt} = \frac{d\tilde{B}}{dt} = j.[\tilde{A}]$$

For the base case (generally temperature of 300 K), A_0 and E_0 have been obtained experimentally and are used to determine reaction rates in different temperatures. From collision theory, for gases, A is directly related to the square root of temperature (Seinfeld & Pandis, 2006). E is the required energy for reaction to be completed and is independent of the ambient temperature. Therefore:

$$A = A_0(\frac{T}{T_0})^{\frac{1}{2}} \quad (7)$$

Replacing A in the reaction rate formula (6) yields

$$k = A_0(\frac{T}{T_0})^{\frac{1}{2}}.e^{-\frac{E_0}{RT}} \quad (8)$$

This parameterization will be used for the reaction rates wherever experimental data is not available. Atmospheric reactions and their corresponding rates can be found in references (Seinfeld & Pandis, 2006; Atkinson, et al., 2004).

2.2.2. Parameterization of photolysis rate

Photolysis rate is normally based on quantum yield and cross section of a reaction (see (Atkinson, et al., 2004), and references therein). However, here, we used the parameterized rate of the

photochemical reactions. Each photolysis reaction is a function of the zenith angle (z) and can be estimated from parameterization type proposed by Collins et al. (Collins, Stevenson, Johnson, & Derwent, 1997).

$$j = \alpha e^{-\beta.\sec(z)} \quad (9)$$

Four main photochemical reactions were considered in this work and two constants (α, β) were estimated based on the available data for photolysis reaction rate of 15 degrees zenith angle (Collins, Stevenson, Johnson, & Derwent, 1997) and zenith sun (Seinfeld & Pandis, 2006) at 0.5 *km* altitude (Table 2).

Reaction	$Z = 0^{\circ}$	$Z = 15^{\circ}$
$j_{O_3+hv\rightarrow O}$	6.5×10^{-4}	4.71×10^{-4}
$j_{O_3+hv\rightarrow O_D}$	5×10^{-5}	3.24×10^{-5}
$j_{NO_2+hv\rightarrow O+NO}$	1.39×10^{-2}	9×10^{-3}
$j_{H_2O_2+hv\rightarrow 2OH}$	2.87×10^{-5}	7.98×10^{-6}

Table 2: rate of photolysis reaction of 15 degrees zenith angle (Collins, Stevenson, Johnson, & Derwent, 1997) **and zenith sun** (Seinfeld & Pandis, 2006) **at 0.5 *km* altitude**

2.2.3. Photochemical reactions

The rates of photochemical reactions depend on the solar radiation energy, which primarily relates to the zenith angle. There are different estimates for photolysis rate as a function of altitude; however we considered only the reaction rates near the Earth's surface. In addition to one intermediate reaction of hydrogen peroxide, three main photolysis reactions in the troposphere take place. Ozone dissociates into oxygen atom and oxygen molecule. The oxygen atom may become ground state oxygen (*O*) or excited oxygen (O_D) in the following reactions:

$$O_3 + hv \rightarrow O + O_2 \quad (10)$$

$$O_3 + hv \rightarrow O_D + O_2 \quad (11)$$

The respective reaction rates for these two reactions are:

$$j = 6.45e^{-9.2\sec(z)}(\frac{1}{sec}) \quad (12)$$

$$j = 12.1e^{-12.4\sec(z)}(\frac{1}{sec}) \quad (13)$$

Nitrogen dioxide photodissociation is analogous to photolysis of ozone.

$$NO_2 + hv \rightarrow O + NO \quad (14)$$

$$j = 3439.6e^{-12.4\sec(z)}(\frac{1}{sec}) \quad (15)$$

Hydrogen peroxide is an important intermediate reactant and generates hydroxide, which is highly reactive.

$$H_2O_2 + hv \rightarrow 2OH \quad (16)$$

$$j = 2.75 \times 10^{11}.e^{-36.8\sec(z)}(\frac{1}{sec}) \quad (17)$$

2.2.4. Oxygen reactions

Oxygen atom involves in reactions in a wide range of atmospheric temperature. The first reaction is collision of ground oxygen atom and oxygen molecule by other atmospheric constituents, mainly nitrogen, to produce ozone.

$$O_2 + O + M \rightarrow O_3 + M \quad (18)$$

$$k = 5.5 \times 10^{-34}({}^{T}/_{300})^{-2.6}[N_2]\ (\frac{cm^3}{molecule.sec})\ ^{1} \quad (19)$$

where M represents gases that collide with parents in a reaction and leave the reaction without any change. In atmospheric reactions, M is the mixture of oxygen and nitrogen. The second reaction is the dissipation of ozone when it reacts with the ground oxygen atom.

$$O_3 + O \rightarrow 2O_2 \quad (20)$$

$$k = 8 \times 10^{-12}e^{-\frac{2060}{T}}(\frac{cm^3}{molecule.sec}) \quad (21)$$

The next reaction is the conversion of the excited oxygen atom into the ground oxygen atom by collision, with the other atmospheric constituents.

$$O_D + M \rightarrow O + M \quad (22)$$

$$k_0 = 2.9 \times 10^{-11}[M](\frac{cm^3}{molecule.sec})\ ^{2} \quad (23)$$

Finally, we considered the reaction of excited oxygen atom with H_2O (the only reaction that can produce $\dot{OH}$ in the atmosphere). Some other OH radicals are generated in the following process, but they are also indirect results of this reaction.

$$O_D + H_2O \rightarrow 2\dot{OH} \quad (24)$$

$$k_0 = A_0 = \quad (25)$$

$$2.2 \times 10^{-10}(\frac{cm^3}{molecule.sec})$$

2.2.5. Nitrogen reactions

The only effective reaction in the atmosphere, excluding the photolysis reaction of NO_2, is the dissipation of ozone from the nitric oxide reaction.

$$O_3 + NO \rightarrow NO_2 + O_2 \quad (26)$$

$${}^{E_0}/_{R} = 1500\ \text{K} \quad (27)$$

$$A_0 = 3 \times 10^{-12}\ (\frac{cm^3}{molecule.sec}) \quad (28)$$

2.2.6. Carbon reactions

Carbon monoxide is an important pollutant that is mainly emitted from anthropogenic activities, or more specifically from incomplete combustion. Carbon monoxide reacts with hydroxyl radical, which was generated by the reaction between the oxygen atom and the water molecules.

$$CO + \dot{OH} \rightarrow CO_2 + \dot{H} \quad (29)$$

$$k_0 = A_0 = 1.5 \times 10^{-13}(\frac{cm^3}{molecule.sec}) \quad (30)$$

The hydrogen radicals are highly reactive and simultaneously react with the oxygen molecules and produce Hydroperoxyl radical.

$$O_2 + \dot{H} + M \rightarrow H\dot{O}_2 + M \quad (31)$$

[1] Based on the data provided by Hippler et al. (Hippler, Rahn, & Troe, 1990)

[2] Here, [*M*] is the concentration of N_2 and O_2 mixture

$$k_0 = A_0 = 1.5 \times 10^{-13}\left(\frac{cm^3}{molecule.sec}\right) \quad (32)$$

Hydroperoxyl radical generation is followed by its reaction to nitric oxide and reproduction of nitrogen dioxide.

$$H\dot{O}_2 + NO \rightarrow NO_2 + \dot{O}H \quad (33)$$

$$k = 3.6 \times 10^{-12} e^{\frac{270}{T}} \quad (34)$$

Hydroperoxyl radical also reacts with itself to produce hydrogen peroxide.

$$H\dot{O}_2 + H\dot{O}_2 \rightarrow H_2O_2 + O_2 \quad (35)$$

$$k = 2.2 \times 10^{-13} e^{\frac{600}{T}} \quad (36)$$

Hydrogen peroxide reacts with $\dot{O}H$ in the following manner

$$H_2O_2 + \dot{O}H \rightarrow H\dot{O}_2 + H_2O \quad (37)$$

$$k = 2.9 \times 10^{-12} e^{-\frac{160}{T}} \quad (38)$$

The termination reaction for this cycle is the production of nitric acid.

$$\dot{O}H + NO_2 + M \rightarrow HNO_3 + M \quad (39)$$

$$k = 3.3 \times 10^{-30} \left({}^{T}/_{300}\right)^{-3} [N_2] \quad (40)$$

3. Simulation

The model is simulated using the STELLA software based on the stock and flow method (Ford, 2009). One stock is defined for each gaseous component with several inflows and outflows. The inflows and outflows represent the rate of production or generation and dissipation or dispersion of a pollutant (Figure 1). Simulation was run for the city of Los Angeles from 12:00 PM (hour 0) of August 21 to 12:00 PM (hour 96) August 25. We used TMY3 data for wind velocity (m/s), temperature (K) and zenith angle (degrees) for the four days (National Solar Radiation Data Base, 2011). The desired time interval to record the concentration of pollutants was one second. However due to the software's computational limitation, an 18 seconds interval was chosen. To increase the accuracy of the simulation, the fourth order Runge-Kutta discretization method was used. Other options were second order Runge-Kutta and Euler explicit that both produce larger errors (Hirsch, 2007; Roger A. Pielke, 2002). Nitric oxide and nitrogen dioxide anthropogenic emissions were considered to have the ratio of 10:1 (David A. Valler, 2012). Emission of carbon monoxide considered to be four times more than total NO_x emission (Air Resources Board, 2009). Diurnal variation of anthropogenic emission assumed to be identical in each day of simulation. According to references (Gao, 2007; Sailor & Lu, 2004; Gantt, Meskhidze, Zhang, & Xu, 2010), anthropogenic heating and pollution emissions in Los Angeles start to increase from morning and reach their peak before noon. As illustrated in Figure 2, after the constant emission generation during the day, heating and pollution emission decrease eventually, by decreasing anthropogenic activities. This assumption is logical because in summertime and during working days anthropogenic activities and cooling load gradually reach their peak value when temperature increases. Wind velocity, temperature, zenith angle and relative humidity of Los Angeles were used as the inputs of the simulations (Figure 3).

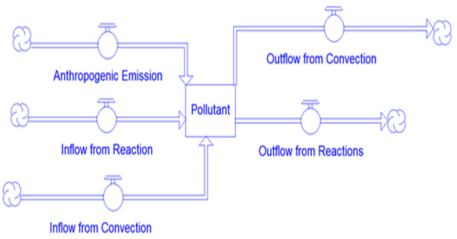

Figure 1: Schematic of stock and flows for a pollutant in STELLA software

4. Results and Discussion

The first cycle (hour 0 to 24) of different calculated variables were ignored, according to the spin-up cycle of the simulation. Qualitative change in the anthropogenic emissions and the photochemical reaction rates were then observed (Figure 4 and 5) to verify the proposed model. As illustrated in Figure 5, nitric oxide was consumed as soon as it was produced from the human activities or generated from the chemical reactions. The concentration of nitric oxide is much less than the other pollutants and its maximum value was less than 5 ppb. Carbon monoxide and nitrogen dioxide had similar periodic behavior and the concentration of these components was proportional to the rate of their emission. Nitrogen dioxide had a sharp increase when the zenith angle became small, and had a gradual decrease after passing its peak value. Concentration of carbon monoxide increased and decreased smoothly and periodically. Furthermore, wind is the critical parameter in this simulation which speeds up the process of pollution dispersion. The reaction rates of pollutants in nighttime were small, there is no photochemical reaction. As a result, when running the model for a case in which the wind velocity was zero, persistent accumulation of the pollutants and a negligible dissipation from the chemical reactions in nighttime captured.

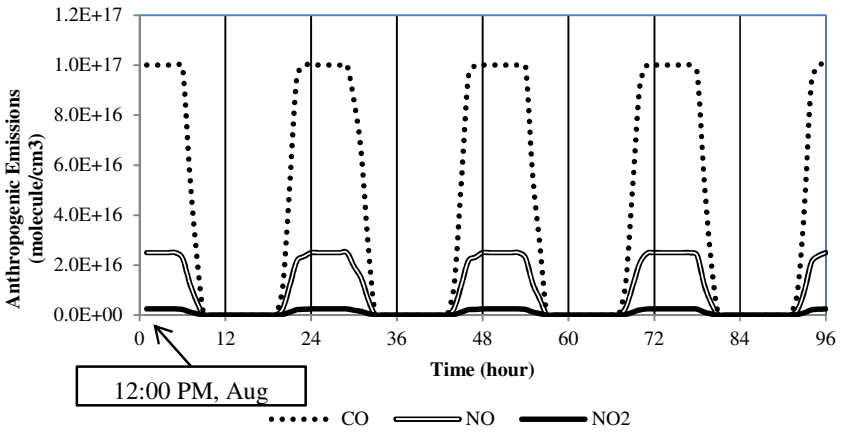

Figure 2: Anthropogenic emissions of NO_2, NO and CO ($^{molecule}/_{cm^3}$) as a function of time (hour)

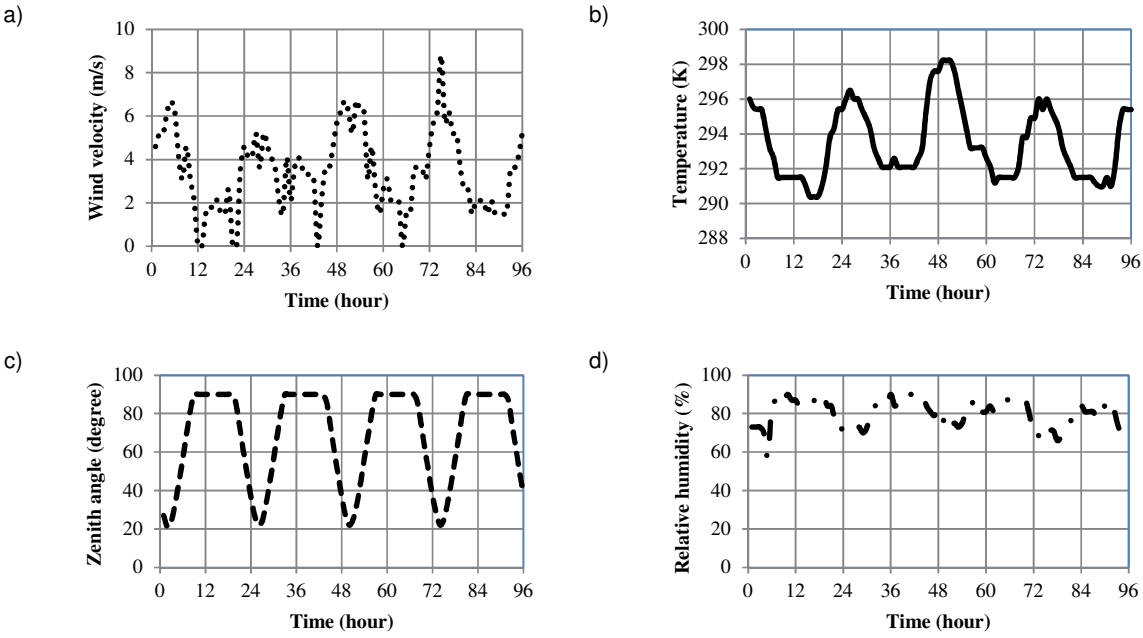

Figure 3: a)Wind velocity ($^{m}/_{s}$), b)Temperature (K), c)Zenith angle (degree), and d)Relative humidity (%) of Los Angeles in specified period of time (National Solar Radiation Data Base, 2011)

Verification of the model was based on variation of the concentration of nitrogen dioxide and nitric oxide, and the rate of photochemical reactions. In a real case, the maximum concentration of nitric oxide occurs in the morning followed by an increase in the concentration of nitrogen dioxide (Austin, 1999). Simulation results qualitatively followed the same pattern, however, the maximum concentration of NO_2 occurred a couple of hours later than the expected time. Figure 5 illustrates the reaction rates of the four photochemical reactions, considering as the other parameters, to evaluate the model. All the reaction rates had their maximum value at the exact time when the zenith angle was minimum. This result clearly shows that the photolysis processes in this group of the reactions were captured, accurately. The small increase in the hydroproxyl reaction rate is due to the small reaction rate coefficient of the reactions that produced hydroproxyl.

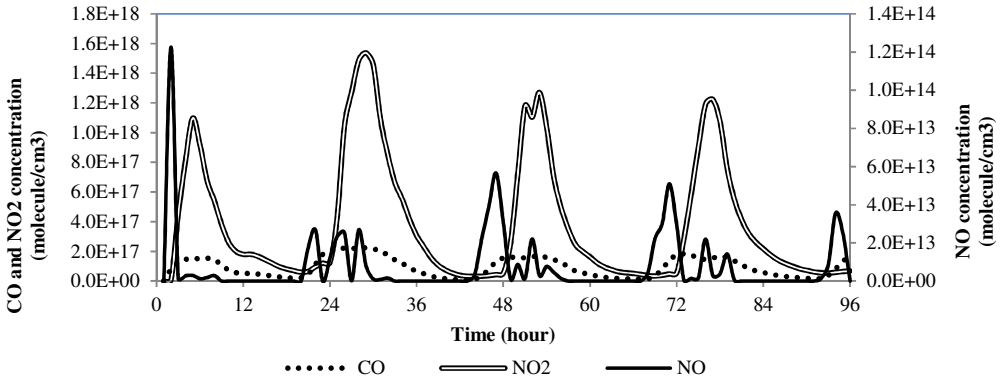

Figure 4: Time series CO, NO_2 and NO concentration ($^{molecule}/_{cm^3}$) variation

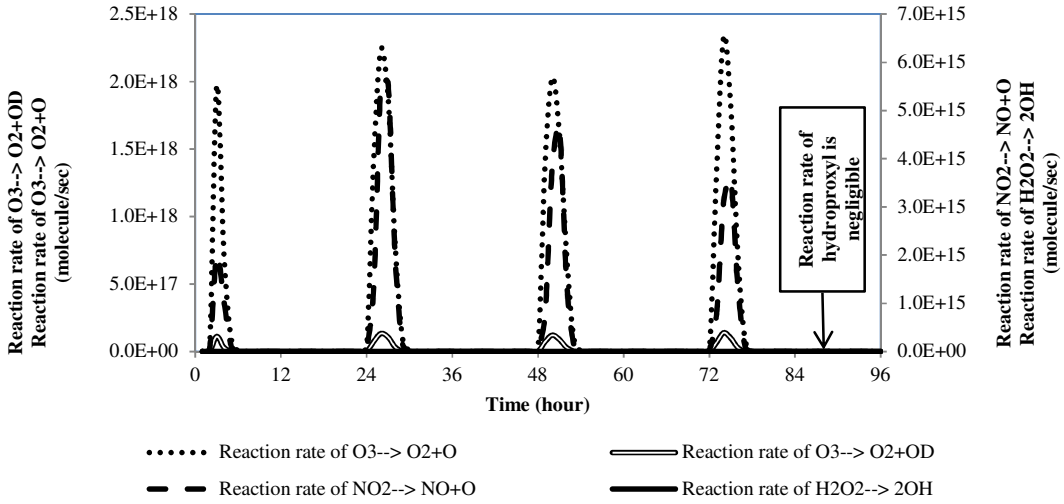

Figure 5: Cyclic changes of photochemical reaction rates

The most important result of this modeling is variation of the ozone concentration during the simulation period (Figure 6). The ozone concentration started to grow rapidly after a lag when temperature started to increase. Thereafter, the ozone concentration got its maximum value as temperature reached its peak. The temperature increase in simulation of the late summer episode was accompanied by the least value of solar zenith angle, which had direct effect on the photolysis rate as discussed in section 3.2. In the stagnant case the ozone concentration was almost constant, indicated that the net rate of ozone generation is negligible. The minimum concentration of ozone occurred right before noon and it was about $1.2 \times 10^{17}(\frac{molecule}{cm^3})$, or $40(ppb)$. The maximum concentration of ozone was about $7.5 \times 10^{18}(\frac{molecule}{cm^3})$ or $300(ppb)$, and after a few hours it started to decrease smoothly. Finally, we determined the sensitivity response of the ozone concentration to the temperature variation by keeping the relative humidity, wind velocity and anthropogenic emission constant. The temperature was the only parameter changed to 0.9 and 1.1 of its initial value. As a result, by increasing the temperature, the ozone concentration reduced and vice versa (Figure 7). This result is a consequence of the rate coefficient of the reaction (18), the only reaction that produced ozone, which was inversely proportional to the temperature. However, all the other reaction rate coefficients were proportional to the temperature. Therefore, to improve the ozone concentration dependence on temperature, volatile organic compounds and the other related reactions should be considered. The role of VOCs in ground-level ozone generation is to form radical intermediates converting NO to NO_2. This increase in the NO_2/NO ratio results an increase in the O_3 concentration. Increase in the concentration of NO_2 produced by trees in an urban area enhances the ozone generation before noon. Additionally, increasing temperature also enhances NO_2 generation from the reaction of VOCs.

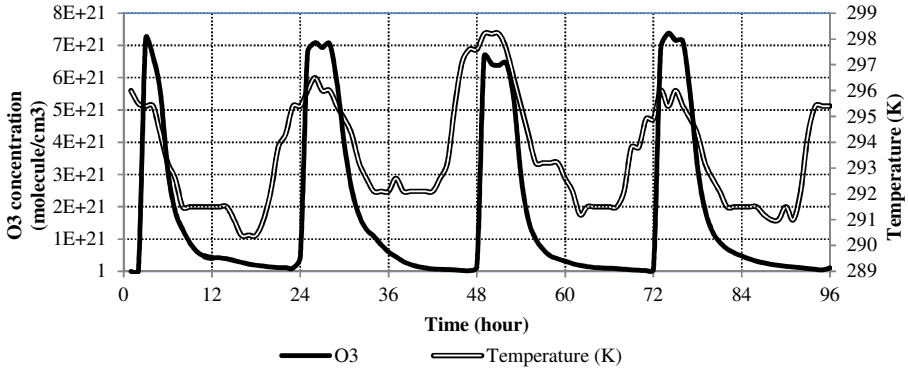

Figure 6: Time series Ozone ($^{molecule}/_{cm^3}$) and Temperature (K) variation

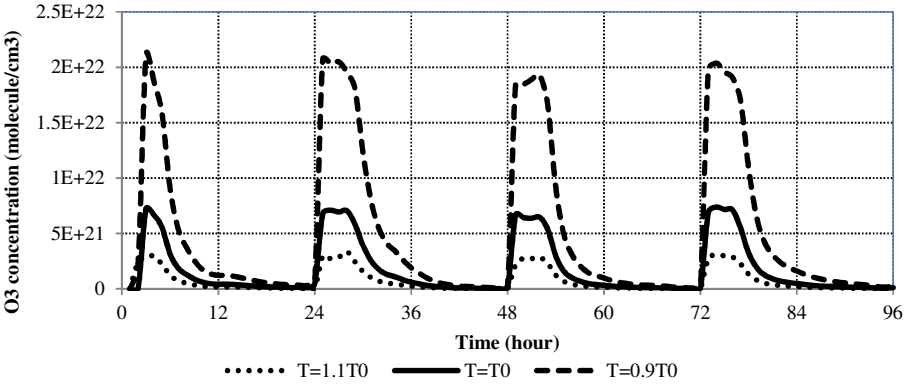

Figure 7: Sensitivity of ozone to the temperature ($T = 0.9T_0$, $T = T_0$and $T = 1.1T_0$)

There are many sources of uncertainties in this modeling:

- The reactions that we considered were based on the major inorganic gaseous components in the atmosphere, introduced in the references (Atkinson, et al., 2004; Seinfeld & Pandis, 2006) and had been used in many other researches. There may be other reactions considered by other references as the main atmospheric reactions, but they're not widely used.
- The STELLA software has some restrictions to simulate the problem due to a limited number of numerical schemes. Its limited number of time intervals was a problem in the simulations. The simulations were performed by 32000 time steps instead of our desired 345000 time steps (in this case each time step would be equal to 1 second).
- These results represent only in a qualitative form and numbers can not represent the exact values of the variables as the hypothetical anthropogenic emission assumption could be much different from the actual case. The actual case of the anthropogenic activities for a short episode was not available.
- Fluctuations, in the peak concentration of different pollutants, were generated by the numerical iteration in some time intervals. The output data presented were digested by omitting irrelevant noises in the system.

5. Summary and conclusion

Many studies used simple models to simulate the air pollution of urban areas as an approach to find the sensitivity response of pollution concentration to temperature, anthropogenic emission, and trace gases. In this paper, we investigated the accuracy of a simple model by considering inorganic atmospheric gaseous constituents. The simulation was performed by the STELLA software for late summer episode of Los Angeles using TMY3 meteorological data, as the input to the model. The Fourth Order Runge-Kutta method for the numerical solution of the problem with 18 seconds time steps was used. For each element or component of the atmosphere that was related to the main reactions, proposed by references (Atkinson, et al., 2004; Seinfeld & Pandis, 2006), one stock defined and appropriate inflows and outflows specified. The inflows and outflows include the generation and dissipation from the chemical reactions. The inflow

and outflow from convection and emission generated from anthropogenic activities are also considered. The reactions and their rate coefficients were derived from previous researches and the overall rate of generation was determined for each component. The photochemical reaction rates were complicated and highly depend on the zenith angle. Therefore, a parameterization was performed and the relationship between the zenith angle and the photochemical reaction rate was defined. The coefficients of the relation between the zenith angle and the photochemical reaction rate are determined based on experimental values for the zenith sun and the zenith angle of 15 degrees. The other chemical reaction rates are mainly extracted from different references and for the cases that data was not available, parameterization was performed. Parameterization was based on collision theory to identify the relationship between reaction rate coefficient and temperature. Pollutants from anthropogenic emissions assumed to be nitric oxide, carbon dioxide and nitrogen dioxide with different amount of emission rate. Simulation was verified based on qualitative comparison of the anthropogenic pollutant's concentrations and the rate of photochemical reactions. Variation of the photochemical reaction rates showed that those reactions captured properly and changes in concentration of NO_2, NO and CO was as expected. Concentration of ozone started to increase after temperature increased, with a lag of a few hours. The maximum concentration was about 300 ppb and ozone concentration fluctuated for a couple of hours until temperature decreased and the zenith angle increased. On the other hand, the ozone concentration decreased smoothly and continued for the rest of the day and even during the night until it reached its minimum value of 50 ppb. Simulations for 0.9 and 1.1 of the base temperature without changing other meteorological parameters resulted in the increase and decrease of the ozone concentration, respectively. By analyzing the sensitivity of the ozone concentration to temperature, we concluded that in this model ozone concentration is decreased by increasing temperature. This result is in contradiction with the other reported models and the experimental data. Consequently, the diurnal variation of the ozone concentration in this model was only because of the photolysis reactions and the corresponding zenith angle. In other words, a model that only consists of the organic gaseous component of atmospheric reactions, the rate of photolysis is a dominant mechanism that describes the quantity of the pollutants. For this reason, these types of models are not able to predict ozone generation of urban areas, properly. There is only one reaction that generates ozone and considering reactions of organic compounds can model ozone generation, accurately. The organic compounds have reaction rates proportional to the temperature and they can increase NO_2/NO ratio, which results in more ground state oxygen atom that follows by the more ozone generation. Finally, we concluded that in order to model the ozone generation of an urban area organic compounds have to be considered as well as inorganic atmospheric constituents.

Nomenclature

A	Collision frequency or pre-exponential factor (unit depends on reaction's type)
A_0	A at 300 K
E	Activation energy of reaction (*J*)
E_0	E at 300 K (*J*)
j	Photolysis rate ($\frac{1}{sec}$)
k	Reaction rate (unit depends on type of a reaction)
R	universal gas constant ($\frac{J}{mol.K}$)
T	Temperature (*K*)
Z	Zenith angle (degrees)

Greek letters:

α	Pre-exponential factor in photochemical reaction ($\frac{1}{sec}$)
β	Exponential power in photochemical reaction

References:

United Nation Information Service. (2004). (United Nation) Retrieved from http://www.unis.unvienna.org/unis/pressrels/2004/pop899.html

National Solar Radiation Data Base. (2011). Retrieved from http://rredc.nrel.gov/solar/old_data/nsrdb/1991-2005/tmy3/by_state_and_city.html#Top

Air Resources Board, C. E. (2009). *2008 Estimated Annual Average Emissions*. (Air Resources Board of California Environmental Protection Agency) Retrieved 07 06, 2012, from http://www.arb.ca.gov/app/emsinv/emssumcat_query.php?F_DIV=-4&F_DD=Y&F_YR=2008&F_SEASON=A&SP=2009&F_AREA=CO&F_CO=19

Alba Webb, J., Parmenter, B., Allen, D. T., & Mc Donald-buller, E. (2008,). The Impacts of Urbanization on Emissions and Air Quality: Comparison of Four Visions of Austin, Texas. *Environ. Sci. Technol., 42,*, 7294–7300.

Atkinson, R., Baulch, D. L., Cox, R. A., Crowley, J. N., Hampson, R. F., Hynes, R. G., . . . Troe, J. (2004). Evaluated kinetic and photochemical data for atmospheric chemistry: Volume I - gas phase reactions of Ox, HOx, NOx and SOx species. *Atmos. Chem. Phys., 4*, 1461-1738.

Austin, J. (1999). *Day-of-Week Patterns in Diurnal Profiles of NO2/NO Ratios Los Angeles Area, 1989 through 1998*. Planning and Technical Support Division California Air Resources Board. Retrieved from

www.arb.ca.gov/research/weekendeffect/NONO2ratio092299.doc

Baldwin, A. C., Barker, J. R., Golden, D. M., & Hendry, D. G. (1977). Photochemical Smog. Rate Parameter Estimates and Computer Simulations. *The Journal of Physjcal Chemistry, Vol. 1, No. 25, , 81*(25), 2483-2492.

Canadian Centre for Occupational Health and Safety. (1998, 01 15). *Health Effects of Ozone*. (Canadian Centre for Occupational Health and Safety) Retrieved 04 06, 2012, from http://www.ccohs.ca/oshanswers/chemicals/chem_profiles/ozone/health_ozo.html

Carter, W. P., Wine, A. M., Darnall, K. R., & N. Pitts, J. (1979). Smog Chamber Studies of Temperature Effects in Photochemical Smog. *Environmental Science & Technology*, 1094-1100.

Collins, W. J., Stevenson, D., Johnson, C., & Derwent, R. (1997). Tropospheric Ozone in a Global-Scale Three-Dimensional Lagrangian Model and Its Response to NOX Emission Controls. *Journal of Atmospheric Chemistry, 26*, 223–274.

David A. Valler, J. (2012). *The Physics and Chemistry of Ozone*. (Feather River Air Quality Management District) Retrieved 07 07, 2012, from http://www.fraqmd.org/OzoneChemistry.htm

Dickerson, R. R., Kondragunta, S., Stenchikov, G., Civerolo, K. L., Doddridge, B. G., & Holben, B. N. (1997). The Impact of Aerosols on Solar Ultraviolet Radiation and Photochemical Smog. *SCIENCE , 278*, 827-830.

Duh, J.-D., Shandas, V., Chang, H., & George, L. A. (2008). Rates of urbanisation and the resiliency of air and water quality. *SCIENCE OF THE TOTAL ENVIRONMENT, 400*, 238–256.

EPA. (2004). *Community Air Screening How to- Manual.* Washington. DC.: United States Environmental Protection Agency. Retrieved from http://www.epa.gov/oppt/cahp/pubs/community_air_screening_how-to_manual.pdf

EPA. (2011, November 4). *Air Pollution Emissions Overview*. Retrieved from United States Environmental Protection Agency: http://www.epa.gov/oar/oaqps/emissns.html

Eyring, V., & et al. (2006). Assessment of temperature, trace species, and ozone in chemistry-climate model simulations of the recent past. *JOURNAL OF GEOPHYSICAL RESEARCH, 111*.

Ford, A. (2009). *Modeling the Environment* (2 ed.). Washington DC: Island Press.

Gantt, B., Meskhidze, N., Zhang, Y., & Xu, J. (2010). The effect of marine isoprene emissions on secondary organic aerosol and ozone formation in the coastal United States. *Atmospheric Environment, 44*, 115–121.

Gao, H. O. (2007). Day of week effects on diurnal ozone/NOx cycles and transportation emissions in Southern California. *Transportation Research, 12* , 292–305.

Hess, G., Carnovale, F., Cope, M., & Johnson, G. M. (1992). The evaluation of Some Photochemical Smog Reaction Mechanisms-1. Temperature and Initial Composition Effects. *Atmospheric Environment, 26A*(4), 625-641.

Hippler, H., Rahn, R., & Troe, J. (1990). Temperature and pressure dependence of ozone formation rates in the range 1–1000 bar and 90–370 K. *Journal of Chemical Physics, 93*(9), 6560-6570 .

Hirsch, C. (2007). *Numerical Computation of Internal and External Flows.* Burlington: John Wiley and Sons.

Jacobson, M. Z. (2001). GATOR-GCMM: 2. A study of day- and nighttime ozone layers aloft, ozone in national parks, and weather during the SARMAP Field Campaign. *J. Geophys. Res., 106*, 5403-5420.

Jacobson, M. Z. (2001). GATOR-GCMM: A global through urban scale air pollution and weather forecast model. 1. Model design and treatment of subgrid soil, vegetation, roads, rooftops, water, sea ice, and snow. *J. Geophys. Res., 106*, 5385-5402.

Li, Y., Li, Y., Zhou, Y., Shi, Y., & Zhu, X. (2012). Investigation of a coupling model of coordination between urbanization and the environment. *Journal of Environmental Management, 98*, 127-133.

Moore, M., Gould, P., & Keary, B. S. (2003). Global Urbanization and Impact on healt. *Int. J. Hyg. Environ. Health, 206*, 269 - 278.

Roger A. Pielke, S. (2002). *Mesoscale Meteorological Modeling.* San Diego: Academic Press.

Sailor, D. J., & Lu, L. (2004). A top–down methodology for developing diurnal and seasonal anthropogenic heating profiles for urban areas. *Atmospheric Environment, 38* , 2737–2748.

Seinfeld, J. H., & Pandis, S. N. (2006). *Atmospheric Chemistry and Physics.* John Wiley & Sons.

Song, J., Parmenter, B., McDonald-Buller, Allen, E. C., & T., D. (n.d.). IMPACTS OF URBANIZATION ON BIOGENIC EMISSIONS 1 AND AIR POLLUTANT DEPOSITION. Retrieved 04 06, 2012, from http://www.geo.utexas.edu/climate/Research/Reprints/JAWMA_drydep.pdf

Soubbotina, T. P., & Sheram, K. A. (2000). *Beyond Economic Growth*. Washington, D.C.: the World Bank. Retrieved from http://www.worldbank.org/depweb/beyond/beyond.htm

Stathopoulou, E., Mihalakakou, G., Santamouris, M., & Bagiorgas, H. S. (2008). On the impact of temperature on tropospheric ozone concentration levels in urban environments. *J. Earth Syst. Sci., 117*(3), 227–236.

Taha, H. (1997). Modeling the Effect of Large-ScaleAlbedo Change on Ozone Air Quality in the South Coast Air Basin. *Atmospheric Environment, 31*(11), 1667-1676.

Walcek, C. J., & Yuan, H. H. (1994). Calcualted Influence of Temperature-Related Factors on Ozone Formation in the Lower Tratosphere. *Journal of Applied Meteorology, 34*, 1056-1069.

Wu, S., Mickley, L. J., Jacob, D. J., Logan, J. A., Yantosca, R. M., & Rind, D. (2007). Why are there large differences between models in global budgets of tropospheric ozone? *JOURNAL OF GEOPHYSICAL RESEARCH, 112*.

Zeldin, M., & Meisel, W. (1978). *Use of Meterological Data in Air Quality Trend Analysis.* North Carolina: US Environmental Protection Agency.